

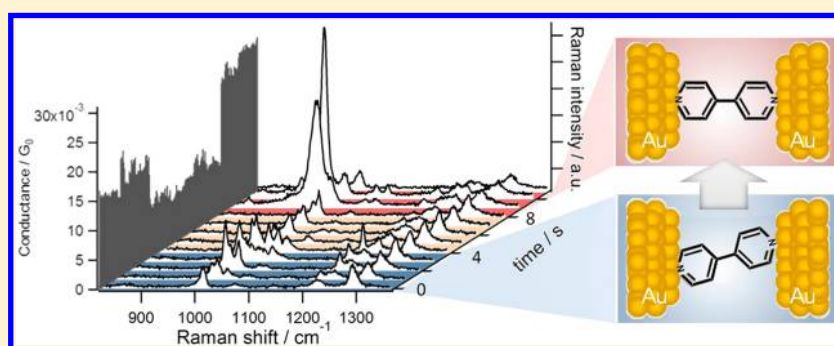
# Single Molecule Dynamics at a Mechanically Controllable Break Junction in Solution at Room Temperature

Tatsuya Konishi,<sup>†</sup> Manabu Kiguchi,<sup>§,\*†</sup> Mai Takase,<sup>†</sup> Fumika Nagasawa,<sup>†</sup> Hideki Nabika,<sup>†</sup> Katsuyoshi Ikeda,<sup>†</sup> Kohei Uosaki,<sup>†</sup> Kosei Ueno,<sup>‡</sup> Hiroaki Misawa,<sup>‡</sup> and Kei Murakoshi<sup>\*,†</sup>

<sup>†</sup>Department of Chemistry, Faculty of Science, Hokkaido University, Sapporo, Hokkaido 060-0810, Japan

<sup>‡</sup>Research Institute for Electronic Science & Nanotechnology Research Center, Hokkaido University, Sapporo, Hokkaido 060-0021, Japan

## Supporting Information



**ABSTRACT:** The in situ observation of geometrical and electronic structural dynamics of a single molecule junction is critically important in order to further progress in molecular electronics. Observations of single molecular junctions are difficult, however, because of sensitivity limits. Here, we report surface-enhanced Raman scattering (SERS) of a single 4,4'-bipyridine molecule under conditions of in situ current flow in a nanogap, by using nano-fabricated, mechanically controllable break junction (MCBJ) electrodes. When adsorbed at room temperature on metal nanoelectrodes in solution to form a single molecule junction, statistical analysis showed that nontotally symmetric  $b_1$  and  $b_2$  modes of 4,4'-bipyridine were strongly enhanced relative to observations of the same modes in solid or aqueous solutions. Significant changes in SERS intensity, energy (wavenumber), and selectivity of Raman vibrational bands that are coincident with current fluctuations provide information on distinct states of electronic and geometrical structure of the single molecule junction, even under large thermal fluctuations occurring at room temperature. We observed the dynamics of 4,4'-bipyridine motion between vertical and tilting configurations in the Au nanogap via  $b_1$  and  $b_2$  mode switching. A slight increase in the tilting angle of the molecule was also observed by noting the increase in the energies of Raman modes and the decrease in conductance of the molecular junction.

## INTRODUCTION

Since it was first suggested that a single molecule might function as an active electronic component, charge transport properties have been investigated for various single-molecule junctions.<sup>1–5</sup> However, it remains difficult to identify the geometrical structure of a single-molecule junction under in situ conditions of flowing current due to the requirement of simultaneous measurements on conductance and photonic or magnetic characteristics, which provide the atomic structure of the single molecule junction. Scanning microprobe methods<sup>6,7</sup> and other techniques<sup>8,9</sup> have provided some information on correlated real-time monitoring of single molecule conductance and molecular orientation at the junction, but they are still not readily applicable to molecular electronic/photonic devices. Surface-enhanced Raman scattering (SERS) is a promising technique for such studies because the Raman modes of the molecule in the nano gap are selectively observed due to the strong electric field across the nanogap electrodes. SERS

provides information on distinct states of electronic and geometrical structure for the single molecule even under the large thermal fluctuation conditions at room temperature. We have found that the observation of single molecules is possible under conditions of bianalyte mixed systems in solution.<sup>10</sup> This demonstrates that the monitoring volume of SERS is less than that of a few nanometer cube in size estimated by electromagnetic theory, and that contributions from additional resonant excitation processes may lead to highly localized enhancement at the single molecule level.<sup>11</sup> Recently, simultaneous measurements on conductance and SERS of a single molecule junction<sup>12–14</sup> were reported. Tian et al. combined SERS and a mechanically controllable break junction method (MCBJ) to observe an enhancement of SERS intensity with decreasing gap size.<sup>14</sup> Ward et al. reported simultaneous

Received: August 10, 2012

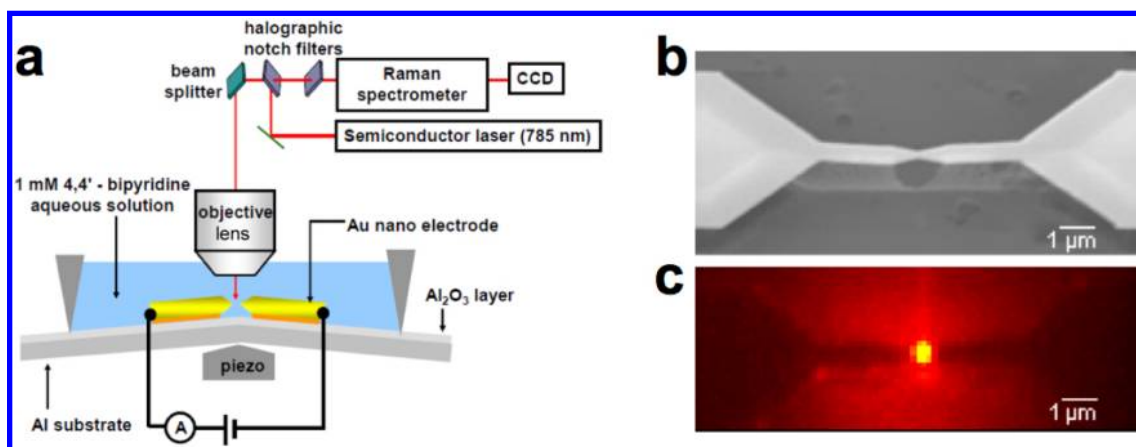


**Figure 1.** (a) Schematic view of the MCBJ-SERS system. (b) SEM image of an Au nanobridge in the MCBJ sample. (c) Raman imaging of the Au nanogap observed at  $1015\text{ cm}^{-1}$ .

measurements of conductance and SERS of a molecular junction where they observed  $b_2$  modes that are not observed in the bulk crystal. Using “fishing mode” tip-enhanced Raman spectroscopy, Liu et al. observed the splitting of a Raman peak for a single molecule junction as well as a shift in peak energy induced by the bias voltage. The peak energy shift was attributed to the change in the binding energy between the molecule and the metal electrodes. While simultaneous SERS and conductance measurement is a powerful technique, the geometrical structure and dynamical motion of the in situ single molecule junction during flowing current are not fully understood. In the present study, we investigated these dynamical aspects of a single molecule junction during simultaneous SERS and conductance measurements.

4,4'-Bipyridine was used because its electron transport properties are well-characterized and will allow conductance measurements to confirm junction fabrication and breaking.<sup>3,13,15–18</sup> Previously documented conductance ranges from  $1.6 \times 10^{-4} G_0$  to  $0.01 G_0$ ,<sup>3,13,15,17,18</sup> The wide range may be due to differing experimental conditions (e.g., solvent, concentrations, bias voltage, and sample treatment).<sup>4,5</sup> We investigated the conductance of the single 4,4'-bipyridine molecule junction using a scanning tunneling microscope (STM) break junction technique under the same experimental conditions as those for the SERS measurements. Observation of conductance indicates formation of a single molecule junction. In the present study, we observed significant modulations in both SERS intensity and the selectivity of the Raman vibrational bands that were coincident with current fluctuations in the single 4,4'-bipyridine molecule junction. Analysis of the Raman bands revealed the geometrical structure and the dynamical motion of the single 4,4'-bipyridine molecule bridging Au electrodes.

## EXPERIMENTAL SECTION

Figure 1a shows a schematic view of the MCBJ-SERS system. The MCBJ sample was fabricated using electron-beam lithography (Figure 1b, see Supporting Information for more detail).<sup>19</sup> In order to reduce substrate fluorescence, aluminum oxide ( $\text{Al}_2\text{O}_3$ ) was utilized as an insulating layer. SERS measurements were carried out in situ by immersing the MCBJ Au nanobridge in an aqueous solution containing 1 mM 4,4' bipyridine. Spectra were obtained with a commercial Raman microprobe spectrometer (Ramascopy, Renishaw), which was modified for near-infrared (NIR) laser light ( $\lambda_{\text{ex}} = 785\text{ nm}$ ). The expanded NIR beam was focused onto the sample using a 100×

water-immersion objective having a numerical aperture of 1.0. The spot size was  $\sim 1\ \mu\text{m}$ , with a tunable intensity of 0.5 mW. Imaging of NIR Raman scattering was performed with an expanded  $30\ \mu\text{m}$  diameter laser beam. The conductance of the Au contact and molecular junction was measured with a DC two-point probe method. The 20 mV bias voltage between the electrodes was provided by a PCI-MIO-16XE-10 AD converter (National Instruments) and the current was measured by a Keithley 6487 picoammeter. The electronic noise level was below  $2 \times 10^{-3} G_0$  under an applied bias voltage of 100 mV.

## RESULT AND DISCUSSION

The self-breaking process<sup>20,21</sup> was utilized for the simultaneous measurements of conductance and SERS. First, the Au nanocontacts having a conductance of  $3 G_0$  were fabricated by controlling substrate bending with a stacked piezo-element; the contacts spontaneously broke from thermal fluctuations and current-induced forces. Since the piezo element was fixed, the imaging and spectra were in focus during the SERS measurements. Before the Au nanobridge was broken, the intensity of the Raman scattering was not detected for an exposure time of less than a few seconds. A single molecule junction was prepared by breaking the Au nanobridge,<sup>22</sup> after which the Raman signal was detected at the nanogap. Figure 1c depicts Raman imaging of the Au nanogap at  $1015\text{ cm}^{-1}$ , which corresponds to the 4,4'-bipyridine ring-breathing vibrational mode.<sup>23–25</sup> While the intensity of the Raman scattering varied with the samples, intense Raman scattering due to the 4,4' bipyridine molecule was observed at the gap. When the 4,4'-bipyridine molecule was absent in the solution, Raman scattering was not detected, indicating that the Raman signal was solely due to the molecule in the gap, and was not due to the bare Au electrodes or other contaminants. The intensity of the scattering was very sensitive to the polarization direction of the 785 nm laser light. Polarization parallel to the Au nanogap resulted in the most intense scattering signal at the nanogap, indicating that the 4,4'-bipyridine signal was due largely to the localized surface plasmon excitation of the Au nanoelectrodes (Figure S2 in Supporting Information).<sup>12,26,27</sup> The SERS spectrum was not affected by the conductance measurement. There were no changes in SERS spectra created by switching the bias off or on during the formation of a single molecule junction.

SERS spectra were significantly dependent upon junction conductance. Figure 2a shows the typical time course of the

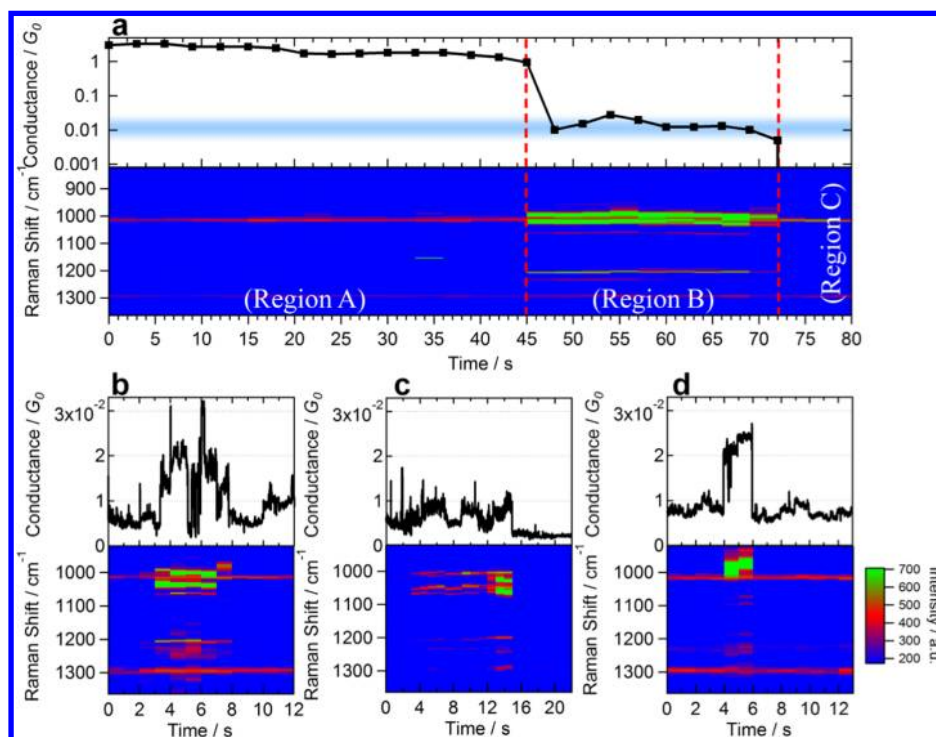


**Figure 2.** (a) Time course of the conductivity and SERS spectra during breaking of the junction. (b–d) Time course of the conductivity and SERS spectra for different molecule junctions at the single molecule conductance regime.

conductivity and the SERS spectra observed during breaking of the junction. The conductance had a plateau at one unit of  $G_0$ , indicating the formation of an Au monatomic contact (Region A in Figure 2a). Another conductance plateau appeared at  $0.01 G_0$ . We measured a similar conductance of  $0.01 G_0$  for the single 4,4'-bipyridine molecule junction using the STM break junction technique (see Figure S1 in Supporting Information), which agreed with Xu's and Horiguchi's results<sup>3,17</sup> and was larger than that found elsewhere for the same molecule.<sup>13,15,18</sup> The different conductance values may be due to varying experimental conditions (e.g., bias voltage, breaking speed, and solvent).<sup>4,5</sup> The conductance value of the single 4,4'-bipyridine molecule junction measured here ( $0.01 G_0$ ) was measured under the same experimental conditions as the SERS measurements (see Supporting Information). The appearance of the  $0.01 G_0$  plateau thus corresponded to the formation of a single 4,4'-bipyridine molecule junction (Region B). After the junction was broken, the conductivity dropped to less than  $0.005 G_0$  (Region C). During these conductance changes, the SERS spectra showed very characteristic behavior. Before (Region A) and after (Region C) the formation of the single molecule junction, SERS bands of 4,4'-bipyridine were observed at 1015, 1074, 1230, and 1298  $\text{cm}^{-1}$ . During the presence of the single molecule junction (Region B), additional intense bands were observed at 990, 1020, 1065, and 1200  $\text{cm}^{-1}$ .

Figure 2b–d depicts close-ups of the conductivity time course and coincident SERS spectra for various molecule junctions. In Figure 2b, intense bands appeared at 1001, 1035, 1062, and 1204  $\text{cm}^{-1}$  after 3–7 s. At 7 s, the intense band at 977  $\text{cm}^{-1}$  suddenly appeared and the bands at 1062 and 1035  $\text{cm}^{-1}$  disappeared. In Figure 2c, SERS bands, which were the same as those in Region B of Figure 2a, were observed when the junction conductivity was larger than  $0.01 G_0$ . These bands disappeared after the conductivity dropped below  $0.007 G_0$

because of junction breaking. Correlation of the conductivity fluctuations with the changes in SERS spectra are also shown in Figure 2d. Relatively large changes of more than  $0.01 G_0$  in conductivity led to the observation of a very intense band at 975  $\text{cm}^{-1}$  and characteristic bands at 1186 and 1221  $\text{cm}^{-1}$ . These changes in Raman spectra that depend on the conductance were not observed in the breaking and formation processes of the Au monatomic contact in the absence of a single molecule junction.

Repeated experiments indicated that three types of SERS spectra were observed (Figure 3a). The spectra shown at the bottom of Figure 3a were observed at the Au monatomic contact or just after breaking the junction. The SERS spectra shown at the middle and upper portions of Figure 3a were observed at the formation of a single molecule junction. The

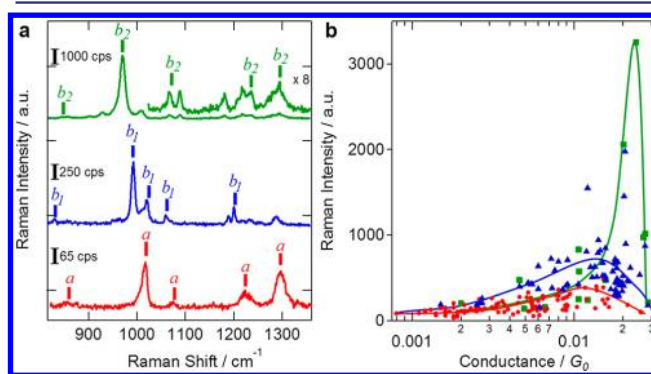


**Figure 3.** (a) Three types of SERS spectra of a single 4,4'-bipyridine molecule junction. Assignment of the totally symmetric *a* mode (red), and the nontotally symmetric *b*<sub>1</sub> mode (blue) and *b*<sub>2</sub> mode (green) are shown as dotted lines. (b) SERS intensity dependence of the *a* (red), *b*<sub>1</sub> (blue), and *b*<sub>2</sub> (green) modes on the conductance of the junction.

SERS bands could be assigned to the vibrational modes of 4,4'-bipyridine on Au, based on a density functional theory calculation at the B3LYP level with a LanL2DZ basis set for Au atoms and a 6-31G\*\* set for other atoms. Accuracy of the mode assignment based on these calculations has been confirmed by a polarized Raman measurement on a single crystal of 4,4'-bipyridine.<sup>24</sup> Assignment of observed SERS bands was confirmed by the number of respective modes derived in the calculation (Table S1 in Supporting Information).

Assigned Raman bands are indicated by bars in Figure 3a. The bands at 1025, 1062, 1217, and 1296  $\text{cm}^{-1}$  (bottom of Figure 3a) can be assigned to totally symmetric *a* modes. Relatively intense bands at 840, 998, 1026, and 1205  $\text{cm}^{-1}$  (middle of Figure 3a) can be assigned to nontotally symmetric *b*<sub>1</sub> modes. The intense 975  $\text{cm}^{-1}$  band (top of Figure 3a) can be assigned to nontotally symmetric *b*<sub>2</sub> modes. Other weak bands at 1072, 1221, and 1299  $\text{cm}^{-1}$  can also be assigned to nontotally symmetric *b*<sub>2</sub> modes. It should be noted that the intensities of the nontotally symmetric *b*<sub>1</sub> and *b*<sub>2</sub> modes were significantly higher relative to totally symmetric *a* mode intensities. In order to investigate the correlation of the single-molecule conductance with the intensity of the Raman signal, more than 700 samples were investigated. Figure 3b depicts the SERS intensity dependence of totally and nontotally symmetric modes on the conductance of the junction. The nontotally symmetric *b*<sub>1</sub> and *b*<sub>2</sub> modes were strongly enhanced around 0.01  $G_0$ , during conductance of the single bipyridine molecule junction, while the intensity of the totally symmetric *a* mode was not sensitive to the conductance of the junction. The present results thus show conclusively that the SERS of nontotally symmetric *b*<sub>1</sub> and *b*<sub>2</sub> modes were induced by the formation of a single molecule junction. By comparing the *b*<sub>1</sub> and *b*<sub>2</sub> modes in more detail, we found that the *b*<sub>2</sub> mode was observed at a higher conductance regime relative to that of the *b*<sub>1</sub> mode.

Selective enhancement of specific vibrational modes has been frequently observed in SERS systems.<sup>11,27–29</sup> In the present case, it is also noteworthy that only Raman signals of bipyridine were observed, whereas signals of water molecules surrounding a single molecule junction, and which did not interact with the Au electrodes, were not detected under the relatively short measurement time. The resulting selective observation of bipyridine molecules supports the previously documented idea that the contribution of the highly localized intense electromagnetic (EM) field by itself is not enough to explain the selective SERS enhancement of a specific vibrational mode.<sup>11,29</sup> The observation of stronger signals for the *b*<sub>1</sub> and *b*<sub>2</sub> modes relative to that for the *a* mode, depending on the single molecule conductance, requires an additional contribution to the Raman enhancement process because the nontotally symmetric modes are described by relatively small nondiagonal terms in the polarizability tensor. If a resonance process via an optical excitation contributes to enhanced Raman scattering, then an additional polarization due to the induced dipole of the excitation changes the observable terms in a Raman tensor, which differ from those in nonresonant cases.<sup>30</sup> The observed nontotally symmetric mode provides information on the orientation of the molecule with respect to the direction of the anisotropic polarization at the single molecule junction, if the direction of the induced dipole caused by the additional resonance is different from that of the highly localized EM field induced by the illumination.

At the Au nanogap, a strong EM field is formed with its polarization direction being parallel to the gap (see Figure S2 in the Supporting Information). Before formation and after breaking the junction, the highly localized electromagnetic field polarizes molecules without an additional excitation resonance (Figure 4a,c). Under this condition, *a* modes are

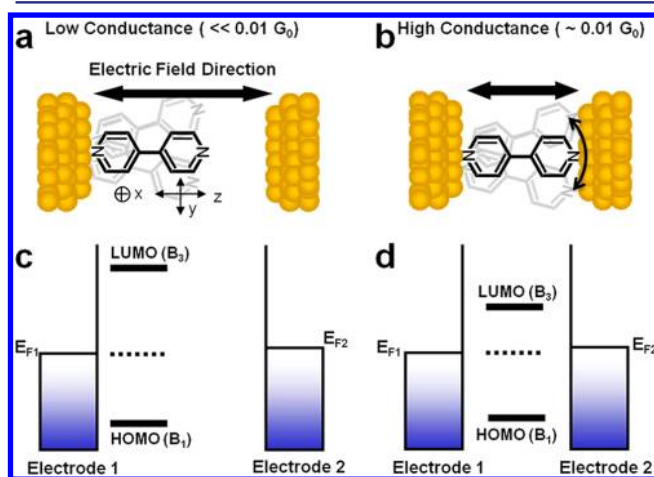


**Figure 4.** (a,b) Possible geometrical structures and (c,d) the corresponding energy diagrams of a single molecule junction.

observed. The orientation of the molecule in the anisotropic EM field can be determined by the relative intensities of *a* mode bands.<sup>24</sup> However, during the presence of a single-molecule junction, an additional excitation of the junction may occur via an energy shift of the molecular orbitals due to hybridization of molecular and metal electronic states.<sup>31</sup> Because of the energy shift of the HOMO close to the metal Fermi level, excitation of electrons from the metal and/or the molecule to the LUMO with *B*<sub>3</sub> symmetry could occur. This excitation would induce a dipole moment perpendicular to the pyridine ring (*x*-direction shown in Figure 4). In this case, the change in selectivity from the *b*<sub>1</sub> to *b*<sub>2</sub> mode should correlate with the change in the polarization of the EM field from perpendicular to the bipyridine ring (*y*-direction) to parallel to the long axis of bipyridine molecule (*z*-direction), because the nondiagonal terms  $\alpha_{xy}$  and  $\alpha_{xz}$  in the polarizability tensor of bipyridine molecules are responsible for *b*<sub>1</sub> and *b*<sub>2</sub> mode, respectively. Therefore, an intense *b*<sub>2</sub> mode is observed when a molecule vertically bridges the gap. When a molecule becomes tilted, the *b*<sub>1</sub> mode is enhanced. Mode switching of *b*<sub>1</sub> from/to *b*<sub>2</sub> reflects changes in the orientation of molecules parallel or perpendicular to the direction of anisotropic EM fields (Figure 4b,d), respectively.

On the basis of the above discussion, we investigated the time courses of the conductivity and the SERS spectra for the molecular junction, which clearly show the dynamical change in its orientation. Figure 5 depicts as a function of time the conductance and the intensity of *a*, *b*<sub>1</sub>, and *b*<sub>2</sub> modes in the SERS spectra. The *b*<sub>1</sub> mode was observed up to 3 s, and the corresponding conductance value was higher than 0.01  $G_0$ . At 4 s, the *b*<sub>1</sub> mode disappeared together with the sudden drop of conductance below 0.01  $G_0$ . At 7 s, the *b*<sub>2</sub> mode appeared and conductance recovered to the conductance value of the single molecule junction. The observed SERS spectra indicated that the molecule initially bridged the gap with its molecular long axis inclining to the gap direction, after which the molecular junction broke ( $\sim 3$  s), and finally the molecule bridged the gap

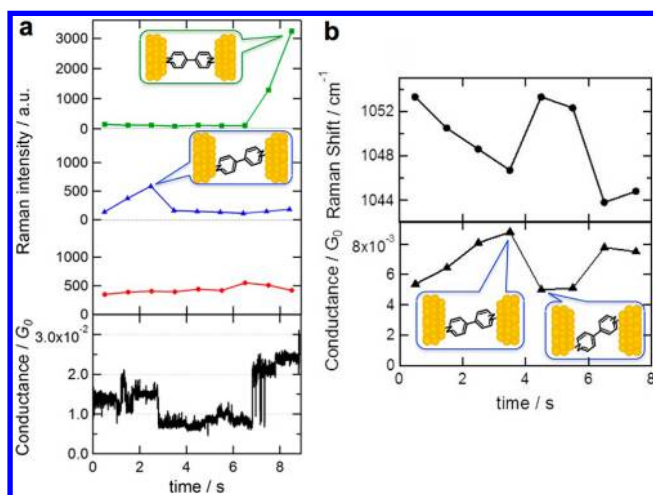


**Figure 5.** (a) Time course of the Raman intensity of the  $a$  mode (red),  $b_1$  mode (blue), and  $b_2$  mode (green) together with the conductance of the molecular junction. (b) Time course of the energy of the  $b_1$  mode of the ring breathing around  $1050 \text{ cm}^{-1}$  and the conductance of the single molecule junction. Schematics of the relevant molecular orientation are shown as insets.

vertically ( $\sim 7$  s). Thus, we could observe the formation and structural change of the molecular junction by SERS and conductance measurements.

In addition to the drastic change in the orientation of the molecule at the junction, a slight change in its orientation was observed through a change in peak energy (wavenumber) and conductance. Figure 5b shows the time-course of conductivity and SERS spectra at the single molecule junction regime. The changes around the  $1050 \text{ cm}^{-1}$  of the ring-breathing  $b_1$  mode coincided with the single molecule conductance fluctuation. The energy of the  $b_1$  mode becomes higher as the conductance becomes smaller. The increase in energy of the  $b_1$  modes observed in Figure 5b,c indicates a slight increase in the angle of the bridging molecule in the Au nanogap. As the bridging molecule becomes tilted in the gap, the strength of the interaction between the molecule and metal electrodes decreases, which leads to the increase in the energy of the internal vibration modes. The fluctuation of the vibrational energy synchronized with the conductance change observed in Figure 5 directly reflects the dynamic motion of the single molecule in the single molecule junction.

Several distinct possibilities should be considered to explain these observations. Concerning the origin of selective Raman mode enhancement, a charge transfer (CT) process that induces vibronic coupling has been considered.<sup>11,29</sup> Excitation of molecule-to-metal or metal-to-molecule CT contributes to the change in the Raman polarizability. Changes in the symmetry of the modes induced by the local environment of the molecules and the metal nanostructure, as well as the surrounding medium, should also be considered. In addition, modulation of selection rules of the optical absorption process at a highly localized EM field must be addressed.<sup>30</sup> It was demonstrated theoretically that forbidden transitions can be allowed by nanostructured EM fields.<sup>32</sup> A breakdown of the selection rules is thus possible, and would contribute to a change in the resonance of the present system. We should consider these possibilities for further precise analysis of the correlation between the Raman observation and the single molecule dynamics.

## CONCLUSIONS

Simultaneous measurements of conductance and SERS were performed for a single 4,4'-bipyridine molecule junction in solution at room temperature, using nanofabricated MCBJ electrodes. The significant changes both in SERS intensity and the selectivity of the Raman vibrational bands correlated with the current fluctuations during breaking and formation of the single molecule junction. We observed motion of the 4,4'-bipyridine between vertical and tilting configurations in the Au nanogap by way of mode switching between  $b_1$  and  $b_2$  in SERS. A slight increase in the angle of the molecule in the gap was observed by the increase in the energy of the Raman modes and a decrease in conductance of the molecular junction. The present study shows that a single molecule at the metal gap produces Raman spectra containing detailed information on the electronic and geometrical structures of the molecule. These observations are based on the phenomena of localized plasmon-enhanced Raman scattering of photons that contain information on the orientation of the single molecules interacting with the metal surface. Thus nonfluorescent molecules such as bipyridine can be used in single-molecule detection, if the electronic states of molecule and metal respond to optical resonance with the localized plasmons. The changes in both intensity and mode switching detected by SERS during a single molecular conductivity measurement provide much more detailed information of a molecular junction than either measurement performed separately. Further detailed studies are required for full understanding of the origins of the changes in the Raman intensity, vibrational energy, and mode selectivity that correlate with the conductance modulations of a single molecule junction.

## ASSOCIATED CONTENT

### Supporting Information

The conductance measurement of the single molecule junction, calculated vibration mode. The material is available free of charge via the Internet at <http://pubs.acs.org>.

## AUTHOR INFORMATION

### Corresponding Author

kei@sci.hokudai.ac.jp; kiguti@chem.titech.ac.jp

### Present Address

<sup>§</sup>Department of Chemistry, Graduate School of Science and Engineering, Tokyo Institute of Technology, 2-12-1 Ookayama, Meguro-ku, Tokyo 152-8551, Japan.

### Notes

The authors declare no competing financial interest.

## ACKNOWLEDGMENTS

This work was partially supported by KAKENHI (Grant-in-Aid for Scientific Research) on Priority Area "Strong Photon-Molecule Coupling Fields (No. 470)" and "Electron transport through a linked molecule in nanoscale (No. 448)" from the Ministry of Education, Culture, Sports, Science, and Technology of Japan.

## REFERENCES

- (1) Aviram, A.; Ratner, M. A. *Chem. Phys. Lett.* **1974**, *29*, 277–283.
- (2) Reed, M. A.; Zhou, C.; Muller, C. J.; Burgin, T. P.; Tour, J. M. *Science* **1997**, *278*, 252–254.
- (3) Xu, B.; Tao, N. J. *Science* **2003**, *301*, 1221–1223.

- (4) Cuevas, J. C.; Scheer, E. *Molecular Electronics*; World Scientific: Singapore, 2010.
- (5) Kiguchi, M.; Takahashi, T.; Takahashi, Y.; Yamauchi, Y.; Murase, T.; Fujita, M.; Tada, T.; Watanabe, S. *Angew. Chem., Int. Ed.* **2011**, *50*, 5708–5711. Kiguchi, M.; Kaneko, S. *Chem Phys Chem* **2012**, *13*, 1116–1126. Kiguchi, M.; Takahashi, T.; Kanehara, M.; Teranishi, T.; Murakoshi, K. *J. Phys. Chem. C* **2009**, *113*, 9014–9017.
- (6) Stipe, B. C.; Rezaei, M. A.; Ho, W. *Science* **1998**, *280*, 1732–1735.
- (7) Qiu, X. H.; Nazin, G. V.; Ho, W. *Science* **2003**, *299*, 542–546.
- (8) Smit, R. H. M.; Noat, Y.; Untiedt, C.; Lang, N. D.; van Hemert, M. C.; van Ruitenbeek, J. M. *Nature* **2002**, *419*, 906–909.
- (9) Kiguchi, M.; Tal, O.; Wohlthat, S.; Pauly, F.; Krieger, M.; Djukic, D.; Cuevas, J. C.; van Ruitenbeek, J. M. *Phys. Rev. Lett.* **2008**, *101*, 046801.
- (10) Sawai, Y.; Takimoto, B.; Nabika, H.; Ajito, K.; Murakoshi, K. *J. Am. Chem. Soc.* **2007**, *129*, 1658–1662.
- (11) Lombardi, J. R.; Birke, R. L. *Acc. Chem. Res.* **2009**, *42*, 734–742.
- (12) Ward, D. R.; Halas, N. J.; Ciszek, J. W.; Tour, J. M.; Wu, Y.; Nordlander, P.; Natelson, D. *Nano Lett.* **2008**, *8*, 919–924.
- (13) Liu, Z.; Ding, S. Y.; Chen, Z.-B.; Wang, X.; Tian, J. H.; Anema, J. R.; Zhou, X. S.; Wu, D. Y.; Mao, B. W.; Xu, X.; Ren, B.; Tian, Z. Q. *Nature Commun.* **2011**, *2*, 1310/1–1310/6.
- (14) Tian, J. H.; Liu, B.; Li, X.; Yang, Z. L.; Ren, B.; Wu, S. T.; Tao, N.; Tian, Z. Q. *J. Am. Chem. Soc.* **2006**, *128*, 14748–14749.
- (15) Quek, S. Y.; Kamenetska, M.; Steigerwald, M. L.; Choi, H. J.; Louie, S. G.; Hybertsen, M. S.; Neaton, J. B.; Venkataraman, L. *Nat. Nanotechnol.* **2009**, *4*, 230–234.
- (16) Hou, S.; Zhang, J.; Li, R.; Ning, J.; Han, R.; Shen, Z.; Zhao, X.; Xue, Z.; Wu, Q. *Nanotechnology* **2005**, *16*, 239–234.
- (17) Horiguchi, K.; Kurokawa, S.; Sakai, A. *J. Chem. Phys.* **2009**, *131*, 104703.
- (18) Zhou, X. S.; Chen, Z. B.; Liu, S. H.; Jin, S.; Liu, L.; Zhang, H. M.; Xie, Z. X.; Jiang, Y. B.; Mao, B. W. *J. Phys. Chem. C* **2008**, *112*, 3935–3940.
- (19) van Ruitenbeek, J. M.; Alvarez, A.; Pineyro, I.; Grahmann, C.; Joyez, P.; Devoret, M. H.; Esteve, D.; Urbina, C. *Rev. Sci. Instrum.* **1996**, *67*, 108–111.
- (20) Yang, Z.; Chshiev, M.; Zwolak, M.; Chen, Y. C.; Di, V. M. *Phys. Rev. B* **2005**, *71*, 041402.
- (21) Todorov, T. N.; Hoekstra, J.; Sutton, A. P. *Phys. Rev. Lett.* **2001**, *86*, 3606–3609.
- (22) Reichert, J.; Ochs, R.; Beckmann, D.; Weber, H. B.; Mayor, M.; Lohneysen, H. V. *Phys. Rev. Lett.* **2002**, *88*, 176804.
- (23) Topaçli, A.; Akyuz, S. *Spectrochim. Acta, Part A* **1995**, *51A*, 633–641.
- (24) Nagasawa, F.; Mai, T.; Nabika, H.; Murakoshi, K. *Chem. Commun.* **2011**, *47*, 4514–4516.
- (25) Zhuang, Z.; Cheng, J.; Wang, X.; Zhao, B.; Han, X.; Luo, Y. *Spectrochim. Acta, Part A* **2007**, *67A*, 509–516.
- (26) Nabika, H.; Takase, M.; Nagasawa, F.; Murakoshi, K. *J. Phys. Chem. Lett.* **2010**, *1*, 2470–2487.
- (27) Ikeda, K.; Suzuki, S.; Uosaki, K. *Nano Lett.* **2011**, *11*, 1716–1722.
- (28) Osawa, M.; Matsuda, N.; Yoshii, K.; Uchida, I. *J. Phys. Chem.* **1994**, *98*, 12702–12707.
- (29) Lombardi, J. R.; Birke, R. L.; Haran, G. *J. Phys. Chem. C* **2011**, *115*, 4540–4545.
- (30) Burstein, E.; Lundqvist, S.; Mills, D. L. the Roles of Surface Roughness. In *Surface Enhanced Raman Scattering*; Chang, R. K., Furtak, T. E., Eds.; Plenum Press: New York, 1982; pp 51–66.
- (31) Li, Z. Y.; Kosov, D. S. *J. Phys. Chem. B* **2006**, *110*, 9893–9898.
- (32) Jain, P.; Ghosh, D.; Baer, R.; Rabani, E.; Paul, A. *Proc. Natl. Acad. Sci. U.S.A.* **2012**, *109*, 8016–8019.